Journal of Molecular Spectroscopy 271 (2012) 10–14

Contents lists available at SciVerse ScienceDirect

Journal of Molecular Spectroscopy

journal homepage: www.elsevier.com/locate/jms

High resolution laser excitation spectroscopy of barium monosulfide

Gang Li [a,*], Jin-Guo Wang [a], Peter F. Bernath [a,b]

[a] Department of Chemistry, University of York, Heslington, York YO10 5DD, UK
[b] Department of Chemistry and Biochemistry, Old Dominion University, Norfolk, VA 23529, USA

ARTICLE INFO

Article history:
Received 30 September 2011
Available online 4 November 2011

Keywords:
Barium monosulfide
Laser excitation spectroscopy
Equilibrium constants

ABSTRACT

High-resolution spectra of BaS were recorded using laser excitation spectroscopy. BaS molecules were synthesized in a Broida-type oven. The observed rotationally-resolved spectrum of BaS in the 12 100–12 765 cm^{-1} spectral range contains the 2-1, 3-1, 3-2, 4-2, 5-2, 5-3 vibrational bands of the $A'^1\Pi$–$X^1\Sigma^+$ transition and the 4-1, 5-1, 5-2 vibrational bands of the $a^3\Pi_1$–$X^1\Sigma^+$ transition. Approximately 1000 lines of the $A'^1\Pi$–$X^1\Sigma^+$ transition and 600 lines of the $a^3\Pi_1$–$X^1\Sigma^+$ transition for the main isotopologue $^{138}Ba^{32}S$ (67.5% natural abundance) were measured. Rotational and vibrational parameters were derived for the $A'^1\Pi$ and $a^3\Pi_1$ states.

1. Introduction

The interest in solid BaS dates back to the early 17th century when a white mineral (barite, $BaSO_4$) was found near Bologna, Italy. After reduction of the powder with charcoal at high temperature to form at least some BaS, the material ('Bologna stone') became phosphorescent. Bologna stone drew the attention of various of alchemists, chemists and philosophers due to its 'magic' property of emitting light in darkness for hours [1]. It was an important object for scientific study of luminescent phenomena [2]. In modern chemistry, the inorganic compound BaS has been used as precursor to other barium compounds including $BaCO_3$ and the pigment lithopone, $ZnS/BaSO_4$ [3]. Barium sulfide also finds application as an optical material [4–6]. Alkaline earth metal sulfides including BaS have drawn the attention of spectroscopists for their potential astrophysical applications [7].

The electronic states of diatomic oxides and sulfides have been extensively studied in the past few decades [8–14]. Studies of the low-lying electronic states of BaS may be traced back to 1937 when Mathur observed only a region of continuous absorption and measured its latent heat of vaporization [15]. In 1971, Barrow et al. rotationally analyzed several bands of the $A^1\Sigma^+$–$X^1\Sigma^+$ and the $B^1\Sigma^+$–$X^1\Sigma^+$ transitions using absorption spectroscopy at moderate resolution [8]. Preliminary constants were derived for the $A^1\Sigma^+$ and $B^1\Sigma^+$ states in this work and the $A^1\Sigma^+$ state was found to be extensively perturbed by several other low-lying electronic states, which were later identified as the $A'^1\Pi$ and the $a^3\Pi$ states by Cummins et al. [9].

The molecular beam electric resonance technique was used to derive a dipole moment of 10.86 ± 0.02D for the ground state of BaS [12]. The first pure rotational measurement was carried out by Tiemann et al. in 1976 [14]. In this work, the rotational transitions below 70 GHz for the main barium sulfide isotopologue $^{138}Ba^{32}S$ were analyzed. Four years later, Helms et al. extended the measurements to six isotopologues of BaS in the 55–339 GHz spectral range which yielded accurate Durham constants for the ground state [10]. In 1981, Cummins et al. investigated three low lying electronic states, $A^1\Sigma^+$, $A'^1\Pi$ and $a^3\Pi$, using dispersed fluorescence spectroscopy [9]. A cw argon ion laser was used to excite BaS molecules to the $B^1\Sigma^+$ state. Fluorescence spectra of the $B^1\Sigma^+$–$A^1\Sigma^+$, $B^1\Sigma^+$–$A'^1\Pi$ and $B^1\Sigma^+$–$a^3\Pi$ transitions were rotationally assigned. In conjunction with the data from Barrow et al., they were able to analyze the mutual perturbations between the $A^1\Sigma^+$, the $A'^1\Pi$ and the $a^3\Pi$ states and obtain deperturbed constants. Very recently, Janczyk and Ziurys performed a pure rotational study of BaS ($X^1\Sigma^+$) in the frequency range of 355–396 GHz [11]. This work tackled all six isotopologues, $^{138}Ba^{32}S$, $^{137}Ba^{32}S$, $^{136}Ba^{32}S$, $^{135}Ba^{32}S$, $^{134}Ba^{32}S$, and $^{138}Ba^{34}S$ and the results covered the vibrational levels from $v = 0$ to $v = 6$.

In the present paper, we report on high resolution laser excitation spectra of the $A'^1\Pi$–$X^1\Sigma^+$ and $a^3\Pi$–$X^1\Sigma^+$ electronic transitions in the 12 100–12 765 cm^{-1} spectral region. Our new observations contain the 2-1, 3-1, 3-2, 4-2, 5-2 and 5-3 vibrational bands of the $A'^1\Pi$–$X^1\Sigma^+$ transition and the 4-1, 5-1, 5-2 vibrational bands of the $a^3\Pi_1$–$X^1\Sigma^+$ transition. A large number of lines were measured for both transitions for the main isotopologue $^{138}Ba^{32}S$ (67.5%). The measured wavenumbers together with the microwave data from Helms et al. [10], Tiemann et al. [14], sub-millimeter data from Janczyk and Ziurys [11] and the lines for the $A^1\Sigma^+$–$X^1\Sigma^+$ transition from Morbi and Bernath [13] were fitted simultaneously. Spectroscopic constants of the $A'^1\Pi$ and the $a^3\Pi_1$ states

* Corresponding author.
E-mail address: gl525@york.ac.uk (G. Li).

0022-2852/$ - see front matter © 2011 Elsevier Inc. All rights reserved.
doi:10.1016/j.jms.2011.10.003

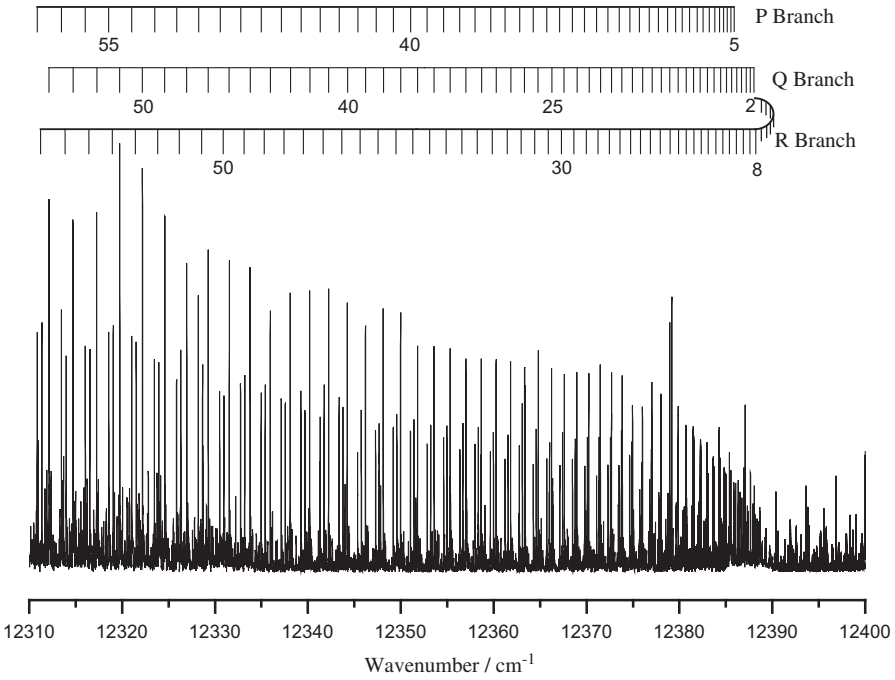

Fig. 1. The laser excitation spectrum of the $v' = 4 - v'' = 2$ band of the $A'^1\Pi$–$X^1\Sigma^+$ transition of BaS. The *J* assignments are labeled on the top of the spectrum.

Table 1
Deslandres table of band origins of the $A'^1\Pi$–$X^1\Sigma^+$ transition of $^{138}Ba^{32}S$.

v'/v''	0		1		2		3
0	12116.0	377.6	11738.4	375.9	11362.5	374.1	10988.4
	259.1		259.1		259.1		259.1
1	12375.1	377.6	11997.5	375.9	11621.6	374.1	11247.5
	257.3		257.3		257.3		257.3
2	12632.4	377.6	12254.7*	375.9	11878.9	374.1	11504.7
	255.4		255.4		255.4		255.4
3	12887.8	377.6	12510.1*	375.9	12134.3*	374.1	11760.1
	253.5		253.5		253.5		253.5
4	13141.3	377.6	12763.7	375.9	12387.8*	374.1	12013.7
	251.7		251.7		251.7		251.7
5	13393.0	377.6	13015.4	375.9	12639.5*	374.1	12265.4*

Note: Bands observed in present study are marked with (*).

Table 2
Franck–Condon factors for the $A'^1\Pi$–$X^1\Sigma^+$ transition of $^{138}Ba^{32}S$.

v'/v''	0	1	2	3	4
0	6.82*E*−06	9.26*E*−05	6.15*E*−04	2.67*E*−03	8.49*E*−03
1	7.00*E*−05	7.96*E*−04	4.35*E*−03	1.51*E*−02	3.70*E*−02
2	3.68*E*−04	**3.47*E*−03**	1.53*E*−02	4.11*E*−02	7.40*E*−02
3	1.33*E*−03	**1.02*E*−02**	**3.53*E*−02**	7.04*E*−02	8.51*E*−02
4	3.67*E*−03	2.27*E*−02	**5.97*E*−02**	8.25*E*−02	5.56*E*−02
5	8.32*E*−03	4.04*E*−02	**7.75*E*−02**	**6.55*E*−02**	1.41*E*−02
6	1.61*E*−02	5.99*E*−02	7.79*E*−02	3.08*E*−02	4.64*E*−04

Observed bands in this study are highlighted in bold.

were obtained and global perturbations were observed for the $A'^1\Pi$ state.

2. Experimental

Barium sulfide was synthesized by reacting barium atoms with carbon disulfide (CS_2) in a Broida-type oven. The setup of a Broida-type oven can be found elsewhere in more detail [16]. Briefly, about 5 g of barium metal was placed in an alumina crucible which was resistively heated by a tungsten wire basket to vaporize the metal. Reagent grade CS_2 vapor from a liquid reservoir was then introduced as the oxidant. In order to prevent formation of BaO, the reservoir was pumped for 2 min prior to the experiment to remove all dissolved oxygen from the CS_2. Argon was used as the carrier gas to entrain Ba vapor into the reaction zone of the oven. The partial pressures of argon and CS_2 used in the experiment were 2.3 Torr and 8 mTorr, respectively. When the oven reached an appropriate temperature a gray chemiluminescent flame approximately 2 cm high with a slightly bluish color was observed after CS_2 vapor was introduced.

A continuous-wave single-mode ring-type titanium:sapphire laser (Coherent 899-29) was used to excite the BaS molecules. The output power of the laser varied from 200 to 500 mW when scanning over the 12 000–12 750 cm^{-1} spectral region. The laser beam was introduced from above the oven into the flame through a Brewster window on top of the oven. Fluorescence could be observed through an infrared viewer during scanning. Maximum fluorescence was achieved by tweaking the partial pressure of argon carrier gas and CS_2 oxidant. The fluorescence was collected and collimated using a lens and was focused into a monochromator (3 mm slit width) which functioned as a band-pass filter. The monochromator was then set at 858.0 nm which was approximately the calculated 1-0 band origin of the $A'^1\Pi$–$X^1\Sigma^+$ transition of BaS. This monochromator position was fixed while the laser was scanned through the spectral range of interest. As the laser was scanned, the optical signal from the monochromator was detected using a photomultiplier tube (PMT). Phase-sensitive detection was realized by chopping the laser beam and feeding the signal from the PMT into a lock-in amplifier which was phase-locked by a reference signal from the mechanical chopper. The output of the lock-in amplifier was then sent to the PC which controlled the laser scanning. Spectra were recorded in 5 cm^{-1} segments at a scan

Table 3
Molecular parameters of BaS from a global least-squares fit.

State	v	T_v/cm^{-1}	B_v/cm^{-1}	$D_v/10^{-8}\times$ cm^{-1}	$q_v/10^{-5}\times$ cm^{-1}
$X^1\Sigma^+$	0	0	0.1031565471(24)	3.066280(39)	∼
	1	377.62824(50)	0.1028405690(53)	3.071952(73)	∼
	2	753.51028(54)	0.1025237193(38)	3.077753(53)	∼
	3	1127.63272(59)	0.1022059039(81)	3.08265(11)	∼
$A^1\Sigma^+$	2	15027.17407(92)	0.0904153(36)	−26.934(278)	∼
	3	15302.17546(58)	0.0913988(20)	−0.530(128)	∼
	4	15579.49514(62)	0.0915935(25)	10.857(191)	∼
	5	15859.72426(71)	0.0914360(35)	17.002(370)	∼
	6	16140.5525(12)	0.0913638(47)	11.652(412)	∼
	7	16421.0228(22)	0.0896986(83)	−36.139(680)	∼
	8	16696.97824(90)	0.0901358(17)	−2.895(79)	∼
	9	16969.88155(80)	0.0899553(19)	4.366(108)	∼
$A'^1\Pi$	2	12632.40645(85)	0.08091439(61)	3.006(11)	−2.234(16)
	3	12887.71574(57)	0.08059585(29)	3.2940(66)	−1.911(14)
	4	13141.37110(61)	0.08028891(23)	3.2474(33)	−2.026(15)
	5	13392.98500(59)	0.08003811(18)	3.5521(25)	−1.9984(77)
$a^3\Pi_1$	4	12710.42715(62)	0.08048896(31)	3.1077(48)	0.984(20)
	5	12962.70210(57)	0.08017305(26)	3.3140(50)	1.2022(96)

Note: Numbers in parentheses are one standard deviation uncertainty in the last digits.

Table 4
Derived equilibrium spectroscopic constants for BaS.

State	T_e/cm^{-1}	ω_e/cm^{-1}	$\omega_e x_e$/cm^{-1}	$B_e/10^{-2}\times$ cm^{-1}	$\alpha_e/10^{-4}\times$ cm^{-1}	R_e (Å)
$A'^1\Pi$	12175.230(785)	260.961(397)	0.9270(476)	8.1577(61)	2.81(13)	2.8217(86)
$a^3\Pi_1$	∼	∼	∼	8.191056(57)	3.1590(98)	2.815919(80)

Note: numbers in parentheses are one standard deviation uncertainty in the last digits.

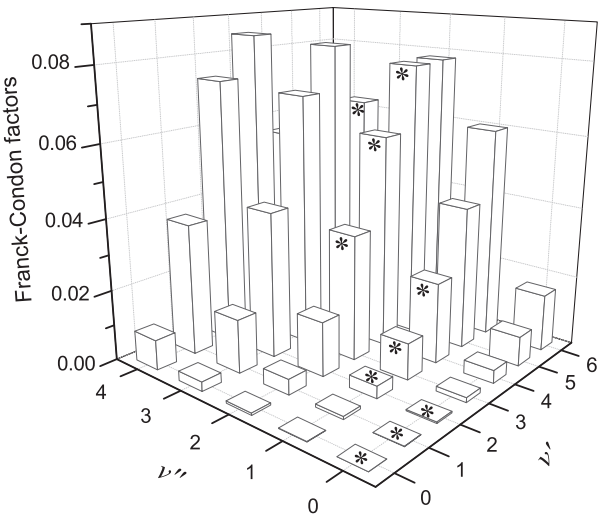

Fig. 2. 3-D bar plot of the Franck–Condon factors of the $A'^1\Pi$–$X^1\Sigma^+$ transition of BaS. The x and y axis, v' and v'', represent upper and lower vibrational levels of the $A'^1\Pi$ and the $X^1\Sigma^+$ state, respectively. All possible transitions within the scanned spectral range are marked with asterisks. The 0-0, 1-0 and 2-0 bands were not found in our spectra due to their small Franck–Condon factors.

speed of 2 GHz per second. In order to calibrate the laser frequency, the laser beam was split and a small portion (5%) was sent to a heated I_2 cell to record I_2 absorption spectra together with BaS spectra. The BaS spectra were observed from 12100 to 12765 cm^{-1}. Fig. 1 shows a section of the recorded laser excitation spectrum of BaS showing the branch structure of the 4-2 band of the $A'^1\Pi$–$X^1\Sigma^+$ transition. The signal-to-noise ratio is estimated to be on the order of 100 for the most intense lines.

In order to analyse the spectra, the line positions were first fitted with a Voigt lineshape function using M. Carleer's WSpectra program [17]. The absolute frequency was calibrated with the absorption spectrum of heated iodine using the I_2 ATLAS database [18]. A Loomis–Wood program was then employed to identify the bands with the J values assigned using lower state combination differences.

3. Results and discussion

3.1. Rotational assignment

Our measurements contain a large number of lines belonging to different isotopologues of BaS. So far only the bands of the main isotopologue $^{138}Ba^{32}S$ (67.5%) have been analyzed. The band structure of a typical band of the $A'^1\Pi$–$X\ ^1\Sigma^+$ transition is illustrated by the 4-2 band shown in Fig. 1. As shown in Fig. 1, the rotational structure of each band of this transition consists of three branches, one P, one Q, and one R branch. The Q branch is the most intense, and the R and P branches have similar intensity. The rotational assignments for lines of the P and R branches were made using lower state combination differences. Sub-millimeter data from Janczyk and Ziurys [11] for the ground state was used to confirm the absolute J assignments. Lines of Q branch were then fitted together with P and R branches using a weighted least-squares fit program called lsqWIN. The rotational term values including the first order centrifugal distortion term used in the least-squares fit are expressed as follows for a $^1\Sigma^+$ and a $^1\Pi$ state, respectively:

$$F_\Sigma(v,J) = B_v J(J+1) - D_v[J(J+1)]^2,$$

and

$$F_\Pi(v,J) = B_v J(J+1) - D_v[J(J+1)]^2 \pm \frac{1}{2} q_v[J(J+1)]^2. \quad (1)$$

In total, six vibrational bands, 2-1, 3-1, 3-2, 4-2, 5-2, and 5-3, of the $A'^1\Pi$–$X^1\Sigma^+$ transition were rotationally analyzed.

As reported by Cummins et al., the $a^3\Pi$ state lies very close to the $A'^1\Pi$ state [9]. The $a^3\Pi$ state may be treated approximately as a Hund's case (c) state where each of the three spin components, $^3\Pi_{0\pm}(F_1)$, $^3\Pi_1(F_2)$ and $^3\Pi_2(F_3)$ is viewed as a separate electronic state. The approximate selection rule $\Delta S = 0$ does not hold strictly when there is a large spin–orbit interaction in heavy molecules such as BaS. For a Hund's case (c) state, only the quantum number Ω, the projection of the total electronic angular momentum about the internuclear axis, is well defined in addition to J and parity; the selection rule is: $\Delta\Omega = 0, \pm 1$.

On account of the above selection rule only the $^3\Pi_{0+}$–$^1\Sigma^+$ and $^3\Pi_1$–$^1\Sigma^+$ sub-bands occur. The structure of these bands is the same as that of singlet bands, namely $^3\Pi_{0+}$–$^1\Sigma^+$ transitions are similar to $^1\Sigma^+$–$^1\Sigma^+$ transitions (one P and one R branch); and $^3\Pi_1$–$^1\Sigma^+$ transitions are similar to $^1\Pi$–$^1\Sigma$ transitions (one P, one R and one Q branch). The observed bands of the $a^3\Pi_1$–$X^1\Sigma^+$ transition of BaS are fairly strong, nearly one third of the strongest $A^1\Pi$–$X^1\Sigma^+$ band. A similar approach as for the $A'^1\Pi$–$X^1\Sigma^+$ transition was used to perform the rotational assignments and rotational constants derived from the least-squares fit are listed in Table 3. No local perturbations were observed (except as noted below) in the bands that were rotationally analyzed.

3.2. Vibrational assignment

The vibrational assignment of the BaS spectra was facilitated by the vibrational parameters reported by Cummins et al. [9]. They have performed a perturbation analysis accounting for the $X^1\Sigma^+ \sim A'^1\Pi \sim a^3\Pi$ mutual perturbations and the deperturbed locations of the $A^1\Pi$ state and the $a^3\Pi_1$ spin component were reported. The observed $A'^1\Pi$ and $a^3\Pi_1$ band origins are shifted from their deperturbed positions by the spin–orbit interaction. Thus, the $A'^1\Pi$ energy should be raised and $a^3\Pi_1$ should be lowered by 91 cm^{-1} in order to predict our observed band origins. Table 1, which is a Deslandres table, shows the calculated band positions of the $A'^1\Pi$–$X^1\Sigma^+$ transition using the customary expression [19] and the vibrational parameters derived by Cummins et al. including the spin–orbit shift. The predict band positions have an accuracy better than 0.5 cm^{-1} and are in good agreement with the observed band heads. According to the Deslandres table, nine vibrational bands of the main isotopologue $^{138}Ba^{32}S$ are within the scanned spectral region of 12 100–12 760 cm^{-1}. However, only six of them were observed. To explain this, Franck–Condon factors were calculated for $v' \leqslant 6$ and $v'' \leqslant 4$ of the $A'^1\Pi$–$X^1\Sigma^+$ transition of BaS (see Table 2). A program called LEVEL [20] was used to accomplish the Franck–Condon calculation with the potentials calculated using the RKR method [21] for both states. The RKR potentials were constructed using the derived vibrational constants in Table 4 for the $A'^1\Pi$ state and Ref. [13] for the $X^1\Sigma^+$ states. Fig. 2 shows the 3-D bar plot of the calculated Franck–Condon factors for the transitions involving $v' = 0$–6 and $v'' = 0$–4. Possible vibrational bands in our experimental region are marked with asterisks. As can be seen in this plot, the Franck–Condon factors for the 0-0, 1-0 and 2-0 bands are much smaller than the others. This explains why these bands were not present in our spectra. It is worth noting that the spectra were recorded over 4 days and the oven conditions changed from time to time so the experimental band intensities are unreliable. However, there is a rough agreement in the intensity trends between the observed spectra and the calculated results. The vibrational assignments of the $a^3\Pi_1$–$X^1\Sigma^+$ bands were also assisted by a Deslandres table calculated using constants from Ref. [9].

In the BaS spectra bands with Q heads at 12 233, 12 265, 12 664, 12 699 cm^{-1} were found. A careful investigation suggested that these bands belong to the $A^2\Pi_{3/2}$–$X^2\Sigma^+$ transition of BaF [22]. It is not clear where the BaF impurity came from, either from the CS_2 solvent or some fluoride salts in the oven from previous experiments.

A final fit was performed varying all the constants for both ground and excited states. Morbi's data [13] were also included in our global fit. Local perturbations were found for Q lines between $J = 64$ and $J = 76$ from the $v = 4$ level of the $a^3\Pi_1$ state to $v = 1$ of the $X^1\Sigma^+$ state. These lines were de-weighted in the global fit. Table 3 presents the rotational constants for all the bands included in our final fit. The values of the Λ-doubling constants, q_v, are irregular in the vibrational levels of the $A'^1\Pi$ state because of interactions with nearby electronic states. Transition wavenumbers and rotational assignments are given in Table S1 as supplementary material. The precision of our line positions is estimated to be 0.002 cm^{-1} for unblended lines. Equilibrium molecular parameters were derived using rotational constants in Table 3. Due to global perturbations the band constants are an irregular function of v; as a consequence there are large errors in the derived equilibrium constants.

4. Conclusions

The present laser spectroscopic investigation of the $A'^1\Pi$ and $a^3\Pi_1$ states of BaS has improved the molecular constants of the two states [9]. The line width of our data is about 0.018 cm^{-1}, limited by Doppler broadening in the flame in the Broida oven. Transitions involving $a^3\Pi_{0+}$ spin component were not observed in this work. Calculations of Franck–Condon factors for the $A'^1\Pi$–$X^1\Sigma^+$ transition were performed, which explained why the 0-0, 1-0 and 2-0 bands were not measured.

High resolution laser excitation spectra from the ground $X^1\Sigma^+$ to the $A'^1\Pi$ and the $a^3\Pi$ states in the 12 100–12 765 cm^{-1} spectral region have been recorded and analyzed. Our new measurements contain the 2-1, 3-1, 3-2, 4-2, 5-2, 5-3 vibrational bands of the $A'^1\Pi$–$X^1\Sigma^+$ transition and the 4-1, 5-1, 5-2 vibrational bands of the $a^3\Pi_1$–$X^1\Sigma^+$ transition. A large number of lines were measured for both transitions for the main isotopologue. The measured wavenumbers together with the microwave data [10,14], sub-millimeter data [11] and lines for the $A^1\Sigma^+$–$X^1\Sigma^+$ transition from Morbi and Bernath [13] were fitted together to obtain improved spectroscopic constants for the $A'^1\Pi$ and $a^3\Pi_1$ states. From the individual band parameters, equilibrium constants were derived for the $A'^1\Pi$ and $a^3\Pi_1$ states. However, these equilibrium constants have large uncertainties due to the global perturbations among the $A^1\Sigma^+$, $A'^1\Pi$ and $a^3\Pi$ states as observed by Cummins et al. [10].

Acknowledgments

Support for this work was provided by the UK Engineering and Physical Sciences Research Council (EPSRC) and the Wild Fund of the Chemistry Department at the University of York.

Appendix A. Supplementary material

Supplementary data associated with this article can be found, in the online version, at doi:10.1016/j.jms.2011.10.003.

References

[1] F. Licetus, Litheosphorus Sive De Lapide Bononiensi Utini: ex typographia Nicolai Schiratti Bologna. University Library of Bologna, Italy, p. 1640.
[2] V.A.S. Marggraf, Chymische Schriften, Band 2. Berlin, p. 1767.
[3] A.F. Holleman, Inorganic Chemistry, Academic Press, San Diego, 2001.
[4] G. Kalpana, B. Palanivel, M. Rajagopalan, Phys. Rev. B 50 (1994) 12318.
[5] R.J. Zollweg, Phys. Rev. 111 (1958) 113.
[6] D.R. Vij, N. Singh, Proc. Soc. Photo-Opt. Instrum. 1523 (1992) 608–612.
[7] A.J. Sauval, J.B. Tatum, Astrophys. J. Suppl. 56 (1984) 193–209.
[8] R.F. Barrow, W.G. Burton, P.A. Jones, Trans. Faraday. Soc. 67 (1971) 902–906.

[9] P.G. Cummins, R.W. Field, I. Renhorn, J. Mol. Spectrosc. 90 (1981) 327–352.
[10] D.A. Helms, M. Winnewisser, G. Winnewisser, J. Phys. Chem. 84 (1980) 1758–1765.
[11] A. Janczyk, L.M. Ziurys, J. Mol. Spectrosc. 236 (2006) 11–15.
[12] C.A. Melendres, A.J. Hebert, K. Street, J. Chem. Phys. 51 (1969) 855–856.
[13] Z. Morbi, P.F. Bernath, J. Mol. Spectrosc. 171 (1995) 210–222.
[14] E. Tiemann, C. Ryzlewicz, T. Torring, Z. Naturforsch. A 31 (1976) 128–130.
[15] L.S. Mathur, P. Roy, Soc. Lond. A Mater. 162 (1937) 83–94.
[16] P.F. Bernath, Science 254 (1991) 665–670.
[17] M.R. Carleer, WSpectra: A Windows (R) Program to Measure Accurately the Line Intensities of High Resolution Fourier Transform Spectra. Ver. 1.1, Université Libre de Braxelles, 2000.
[18] S. Gerstenkorn, J. Vergès, J. Chevillard, Atlas du Spectre d'Absorption de la Molecule d'Iode 11000–14000 cm^{-1}, Laboratoire Aimé Cotton CNRS II 91405 Orsay, France, 1982.
[19] G. Herzberg, Molecular Spectra and Molecular Structure, vol. 1, Krieger, Malabar, Florida, 1989.
[20] R.J. Le Roy, 2007, LEVEL 8.0, University of Waterloo Chemical Physics Research Report CP-663, 2007, <http://scienide2.uwaterloo.ca/~rleroy/level/>.
[21] R.J. Le Roy, 2004, RKR1 2.0, University of Waterloo Chemical Physics Research Report CP-657R, 2004, <http://scienide2.uwaterloo.ca/~rleroy/rkr/>.
[22] T.E. Nevin, Proc. Phys. Soc. 43 (1931) 554–558.